Molecular Pharmacology Fast Forward. Published on November 10, 2009 as doi:10.1124/mol.109.059006

Identification of Dynamin-2-mediated Endocytosis as a New Target of Osteoporosis Drugs, Bisphosphonates

Yuka Masaike, Takeshi Takagi, Masataka Hirota, Joe Yamada, Satoru Ishihara, Tetsu M. C. Yung, Takamasa Inoue, Chika Sawa, Hiroshi Sagara, Satoshi Sakamoto, Yasuaki Kabe, Yasuyuki Takahashi, Yuki Yamaguchi, and Hiroshi Handa

Integrated Research Institute, Tokyo Institute of Technology, Yokohama, Japan (Y.M., S.I., H.H.); Graduate School of Bioscience and Biotechnology, Tokyo Institute of Technology, Yokohama, Japan (T.T., M.H., J.Y., T.M.C.Y., T.I., S.S., Y.K., Y.Y., H.H.); Institute of Medical Science, St. Marianna University School of Medicine, Kawasaki, Japan (C.S.); Institute of Medical Science, University of Tokyo, Japan (H.S.); Research Association for Biotechnology, Yokohama, Japan (Y.T.)

Molecular Pharmacology Fast Forward. Published on November 10, 2009 as DOI: 10.1124/mol.109.059006
This article has not been copyedited and formatted. The final version may differ from this version.

Running title: Bisphosphonates Inhibit Dynamin-2-mediated Endocytosis

Corresponding author: Hiroshi Handa

Integrated Research Institute, Tokyo Institute of Technology

4259 Nagatsuta, Yokohama 226-8503, Japan

Tel: +81-45-924-5872; Fax: +81-45-924-5145; E-mail: handa.h.aa@m.titech.ac.jp

No. of text pages:	24
No. of tables:	0
No. of figures:	7
No. of references:	40
No. of words in Abstract:	150
No. of words in Introduction:	725
No. of words in Discussion:	1,111

Abbreviations: ALN, alendronate; BP, bisphosphonate; CPZ, chlorpromazine; DTT, dithiothreitol; DYN2, dynamin-2; ETI, etidronate; FPPS, farnesyl diphosphate synthase; GED, GTPase effector domain; GGOH, geranylgeraniol; GMA, glycidylmethacrylate; HDV, hepatitis delta virus; LOV, lovastatin; N-BP, nitrogen-containing bisphosphonate; NN-BP, non-nitrogen-containing bisphosphonate; PC, phosphatidylcholine; PH, Pleckstrin homology; PIP_3, phosphatidylinositol (3,4,5)-triphosphate; PMSF, phenymethylsurfonyl fluoride; PRD, proline-arginine-rich domain; SNX9, sorting nexin 9; SUV, small unilamellar vesicle; SV40, simian virus 40; ZOL, zoledronate

Molecular Pharmacology Fast Forward. Published on November 10, 2009 as DOI: 10.1124/mol.109.059006
This article has not been copyedited and formatted. The final version may differ from this version.

ABSTRACT

Nitrogen-containing bisphosphonates are pyrophosphate analogues that have long been the preferred prescription for treating osteoporosis. While these drugs are considered inhibitors of prenylation and are thought to exert their effects on bone resorption by disrupting the signaling pathways downstream of prenylated small GTPases, this explanation appears to be insufficient. As other classes of prenylation inhibitors have recently emerged as potential antiviral therapeutic agents, here we first investigated the effects of bisphosphonates on simian virus 40 and adenovirus infections and, to our surprise, found that viral infections are suppressed by bisphosphonates through a prenylation-independent pathway. By in-house affinity capture techniques, dynamin-2 was identified as a new molecular target of bisphosphonates. Evidence is presented that certain bisphosphonates block endocytosis of adenovirus and a model substrate by inhibiting GTPase activity of dynamin-2. Hence, this study has uncovered a previously unknown mechanism of action of bisphosphonates and offers potential novel use for these drugs.

Molecular Pharmacology Fast Forward. Published on November 10, 2009 as DOI: 10.1124/mol.109.059006
This article has not been copyedited and formatted. The final version may differ from this version.

INTRODUCTION

Bisphosphonate (BP) drugs are pyrophosphate analogues that have long been the preferred prescription for treating resorption-related bone diseases, such as osteoporosis and different types of tumor-induced osteolysis (Heymann et al., 2004; Russell et al., 2007). The mechanism of action of the two types of BP drugs, non-nitrogen-containing BPs (NN-BPs) and nitrogen-containing BPs (N-BPs), are thought to be different. On the one hand, NN-BPs, such as etidronate (ETI), are metabolized into non-hydrolyzable ATP analogues that lead to apoptosis (Frith and Rogers, 2003; Roelofs et al., 2006). On the other hand, N-BPs, such as alendronate (ALN) and zoledronate (ZOL), are considered inhibitors of prenylation, which involves the transfer of an isoprenoid lipid moiety from farnesyl pyrophosphate or geranylgeranyl pyrophosphate onto a C-terminal cysteine residue of proteins with a CXXX box, a characteristic prenylation motif (Frith and Rogers et al., 2003; Roelofs et al., 2006). At the molecular level, N-BPs target farnesyl diphosphate synthase (FPPS), thereby inhibiting the production of the substrates required for prenylation of small GTPases (Coxon et al., 2000; Reszka et al., 1999).

Prenylation inhibitors other than N-BPs have recently emerged as potential antiviral therapeutic agents (Einav and Glenn, 2003). For example, statins such as lovastatin (LOV) inhibit HIV-1 infection through HMG-CoA reductase inhibition (del Real et al., 2004) or respiratory syncytial virus replication by inhibiting RhoA geranylgeranylation (Gower and Graham, 2001). Other examples include the farnesyl transferase inhibitors, such as BZA-5B and FTI-277, which have been shown to inhibit the prenylation of CXXX box found in the hepatitis delta virus (HDV) large delta antigen, leading to suppression of production of HDV particles in different systems (Glenn et al., 1998; Bordier et al., 2002). Theoretically, prenylation inhibitors could also exert antiviral effects on other viruses with key molecules containing the CXXX box, such as the RNA polymerase protein of hepatitis A virus and animal enterovirus (Einav and Glenn, 2003) and the UL32 protein of herpes simplex virus, which has a lower titer accompanied by decreased viral protein synthesis in prenylation inhibitor-treated cells (Farassati et al., 2001).

With respect to N-BPs, there are still few reports on the use of N-BPs in the context

of antiviral therapy. One article showed that N-BPs inhibit the growth of human T-cell leukemia virus type I-infected T-cell lines by inhibiting prenylation through FPPS targeting (Ishikawa et al., 2007), while others report the clinical use of N-BPs to reverse HIV-associated osteoporosis without in-depth discussion of the role of prenylation therein (Negredo et al., 2005; Qaqish and Sims, 2004). Hence there appears to be a potential for dual use of N-BPs as osteopathic and anti-viral drugs, although the underlying mechanisms remain unclear.

Thus far, it has been assumed that N-BPs exert their effects on bone resorption by disrupting the signaling pathways downstream of prenylated small GTPases (Frith and Rogers, 2003). However, this explanation appears to be insufficient, as certain unprenylated small GTPases are found in their active form even in the presence of N-BPs (Dunford et al., 2006), while certain N-BPs exert effects that are not reversible by replenishing cells with substrates for protein prenylation, which suggests that N-BPs may have other cellular targets than FPPS (van Beek et al., 2003). Given the emerging roles of prenylation inhibitors in antiviral therapeutics and the wide but relatively unclear potential of N-BPs therein, here, we carried out an investigation on N-BPs in the context of antiviral therapy. First, we found that simian virus (SV) 40 and adenovirus could be inhibited by N-BPs through a prenylation-independent pathway, which supports the existence of other cellular N-BP targets than FPPS. Hence, to search for this new N-BP molecular target, we used high performance latex beads (glycidylmethacrylate (GMA)-covered GMA-styrene copolymer core beads) that we developed in-house, which is an affinity purification matrix that exhibits chemical and physical stability, high capacity for ligand fixation, low nonspecific protein binding, and high purification efficiency (Shimizu et al., 2000; Sakamoto et al., 2009). Using ALN-conjugated beads, we isolated dynamin-2 (DYN2) and sorting nexin 9 (SNX9) (Lundmark and Carlsson, 2003). Our data show that certain types of N-BPs and NN-BPs target GTPase activity of DYN2, leading to defective scission and release of endocytic vesicles into the cytoplasm. Hence, this study unveils a novel prenylation-independent pathway that is targeted by both types of BPs in inhibiting viral infections and may contribute to widening the scope of use of these efficacious drugs beyond bone diseases.

Molecular Pharmacology Fast Forward. Published on November 10, 2009 as DOI: 10.1124/mol.109.059006
This article has not been copyedited and formatted. The final version may differ from this version.

MATERIALS AND METHODS

Cell culture and reagents. Mouse macrophage cell line RAW264.7 cells were cultured in Dulbecco's modified Eagle's medium containing 10% fetal bovine serum (FBS). Human 293FT cells were cultured in Dulbecco's modified Eagle's medium containing 10% FBS and G418. Human HeLa cells were cultured in minimum essential medium containing 10% FBS.

ALN and ETI were obtained from Asahi Kasei (Shizuoka, Japan), and ZOL was obtained from Novartis Pharma (Tokyo, Japan). Small unilamellar vesicles (SUVs) were prepared essentially as described (Sweitzer and Hinshaw, 1998; Catimel et al., 2009), as follows: Bovine total brain extract (Sigma, Saint Louis, MO, USA) was dissolved in chloroform/methanol (1:2). The solvent was evaporated, and lipid was redissolved in appropriate buffer to a final concentration of 25 or 1 mg/ml by sonication. Similarly, SUVs of defined compositions were prepared using PC or PC/PIP_3 (9:1).

Affinity purification using ALN-conjugated beads. The cytoplasmic extract of RAW264.7 cells was prepared as described (Dignam et al., 1983) and was dialyzed with buffer A (10 mM HEPES [pH 7.9], 10% glycerol, 100 mM KCl, 0.2 mM EDTA, 1 mM dithiothreitol [DTT], 1 mM phenymethylsurfonyl fluoride [PMSF]). ALN was conjugated through the amino group to SGNEGDE beads by incubating 100 mM ALN with 5 mg of SGNEGDE at pH 11 at 70°C for 24 h, essentially as described (Shimizu et al., 2000). For affinity purification, ALN-fixed beads (0.5 mg) were incubated with 250 µl (1 mg protein/ml) of RAW264.7 cell cytoplasmic extract in buffer B (10 mM HEPES [pH 7.9], 10% glycerol, 50 mM KCl, 0.2 mM EDTA, 1 mM DTT, 1 mM PMSF, 0.1% NP-40) at 4°C for 4 h. After the beads were washed five times with buffer B, bound proteins were eluted with buffer C (10 mM HEPES [pH 7.9], 10% glycerol, 300 mM KCl, 0.2 mM EDTA, 1 mM DTT, 1 mM PMSF, 0.1% NP-40). Where indicated, various concentrations of free ALN, ZOL, or ETI were added to the cell extract prior to incubation with the beads. In Fig. 5, ALN-fixed beads (0.25 mg) were incubated 10 µg of recombinant DYN2 proteins in 200 µl of buffer B in the absence or presence of the indicated SUVs for 4 h and processed as above.

Molecular Pharmacology Fast Forward. Published on November 10, 2009 as DOI: 10.1124/mol.109.059006
This article has not been copyedited and formatted. The final version may differ from this version.

Plasmids and recombinant proteins. The cDNA encoding DYN2 was obtained from Prof. Nakayama (Tsukuba Univ., Japan). The DNA fragment encoding VSV-tagged DYN-2 was prepared by PCR using the primers 5'-GGAATTCTACACTGATATCGAAATGAACCGCCTGGGTAAGGCGATGGGCAACCGCGGGAT-3' and 5'-CCCAAGCTTCTAGTCGAGCAGGGACG-3', digested with *Eco*RI and *Hind*III, and ligated into the baculovirus expression vector pFastBac HT-A (Invitrogen, Carlsbad, CA, USA). The DNA fragment encoding SNX9 was obtained from the NIH-3T3 cDNA library using the primers 5'-CGGGATCCATGGCCACCAAGGCTCG-3' and 5'-CCGCTCGAGTTACATAACCGGGAAGCG-3', digested with *Bam*HI and *Xho*I, and ligated into the bacterial expression vector pGEX6T-1 (GE Healthcare, Little Chalfont, Buckinghamshire, UK). For mutational analysis, DNA fragments each encompassing the GTPase domain, the middle domain, the Pleckstrin homology (PH) domain, the GTPase effector domain (GED) and the proline-arginine-rich domain (PRD) of DYN2 were prepared by PCR using appropriate primer pairs and cloned into the bacterial expression vector pGEX6T-1. These domains were defined based on previous studies (Schmid et al., 1998; Artalejo et al., 1997).

Recombinant histidine- and VSV-tagged DYN2 protein was expressed in insect cells according to the manufacture's instructions (Invitrogen, Carlsbad, CA, USA) and purified with Ni-chelate resin (Qiagen, Hilden, Germany). GST-tagged SNX9, DYN2-GTPase, DYN2-middle, DYN2-PH, and DYN2-GED+PRD were expressed in *E. coli* BL21 (DE3) and purified with glutathione Sepharose (GE Healthcare, Little Chalfont, Buckinghamshire, UK), and then GST tag was removed by digestion with PreScission Protease (GE Healthcare, Little Chalfont, Buckinghamshire, England).

GTPase assay. GTPase assay was performed as described (Damke et al., 2001) with some modifications. rDYN2 (0.1 μM) was incubated in the absence or presence of liposomes in GTPase buffer (0.1 M HEPES [pH 7.9], 1 mM EGTA, 1 mM $MgSO_4$, 1 mM DTT, 1 mM sodium azide, 0.2 mM PMSF) at room temperature for 10 min. Next, ALN was added where

Molecular Pharmacology Fast Forward. Published on November 10, 2009 as DOI: 10.1124/mol.109.059006
This article has not been copyedited and formatted. The final version may differ from this version.

indicated, and further incubated for 10 min. Then, 1 mM GTP containing 1 μCi of [α-^{32}P] GTP was added and incubated for 30 min at 37°C. The reactions were stopped by addition of 1 μl of 5% TCA acid, and 1.5 μl aliquots of the samples were spotted on polyethyleneimine-cellulose plates and developed with 0.5 M LiCl/1 M formic acid. The plates were dried and analyzed with a BAS2000 image analyzer (Fuji Film, Tokyo, Japan).

Cellular uptake of transferrin or LDL. HeLa cells serum-starved for 18 h were incubated with 30 μM CPZ for 15 min or with 200 μM ALN, ZOL or ETI for 4 h, and then with 5 μg/ml Alexa-Fluor-546-transferrin or Alexa-Fluor-488-LDL (Invitrogen, Carlsbad, CA, USA) for 15 min. To remove transferrin or LDL that was attached to the cell surface, the cells were washed with ice cold buffer containing 0.2 M acetic acid and 0.5 M NaCl and then with ice-cold phosphate buffered-saline three times. Subsequently, the cells were collected with trypsin/EDTA and subjected to FACS analysis (Becton Dickinson, Franklin Lake, NJ, USA). For fluorescence confocal microscopy, the cells were fixed with 4% formaldehyde for 15 min and visualized under the fluorescence microscope IX-DSU (Olympus, Tokyo, Japan).

Liposome scission assay. Unilamellar liposome was prepared as previously described (Sweitzer and Hinshaw, 1998; Catimel et al., 2009). Solution containing 100 μg of liposome was centrifuged at 12,000 *g* for 10 min, and the pellet was resuspended in buffer containing 25 mM HEPES (pH 7.4), 25 mM KCl, 2.5 mM magnesium acetate, 150 mM potassium glutamate, and 10 mM calcium acetate with or without 400 nM DYN2 and 2 mM ALN, and then incubated at 4°C for 4 h. Subsequently, the samples were further incubated with 400 μM GTP at 37°C for 10 min and then centrifuged at 12,000 *g* for 10 min. Grids were glow-discharged using an ion-coater, and 2 μl of the samples were mounted on the grids, stained with 2% uranium acetate, and observed with a H-7500 electron microscope (Hitachi, Tokyo, Japan) at 80 kV.

Analysis of viral infection. In Fig. 1B and 1C, 293FT cells were incubated with 100 μM ALN or 10 μM LOV in the presence or absence of various concentrations of GGOH for

Molecular Pharmacology Fast Forward. Published on November 10, 2009 as DOI: 10.1124/mol.109.059006
This article has not been copyedited and formatted. The final version may differ from this version.

4h and then infected with recombinant SV40 or adenovirus each carrying the luciferase gene. Two hours post infection, the medium was replaced by fresh medium containing the same concentrations of chemicals, and 18 h post infection, luciferase assay was carried out according to the manufacturer's instructions (Promega, Madison, WI, USA). SV40-luc was constructed by replacing the T antigen gene with the firefly luciferase gene (Nakanishi et al., 2008). AxCA Luc+, recombinant adenovirus expressing the luciferase gene under the control of the CAG promoter was obtained from the RIKEN BioResource center (RDB No. 2453). In Fig. 2A, 2B, and 7B, HeLa cells were incubated with 200 μM BPs or 10 μM LOV in the presence or absence of 10 μM GGOH for 4 h, and then infected with adenovirus for 18 h. Adenovirus infection was analyzed by immunoblotting or immunofluorescence microscopy using anti-E1A monoclonal antibody (NeoMarkers, Fremont, CA, USA). To examine protein prenylation levels, we used anti-Rap1A antibody (Santa Cruz Biotech, Santa Cruz, CA, USA), which reacts with the non-prenylated form of Rap1A. The infected cells were also observed with a H-7500 electron microscope (Hitachi, Tokyo, Japan).

Molecular Pharmacology Fast Forward. Published on November 10, 2009 as DOI: 10.1124/mol.109.059006
This article has not been copyedited and formatted. The final version may differ from this version.

RESULTS

Inhibition of viral infections by ALN through a prenylation-independent pathway. The first step in this study was to test whether a popular N-BP, ALN (Fig. 1A), exerts an inhibitory effect on different types of viruses. LOV, known to inhibit the mevalonate pathway by a different mechanism from ALN, i.e., by blocking HMG-CoA reductase activity, was used as control. Immunoblot analysis of the non-prenylated form of the small GTPase Rap1A showed that under our conditions, prenylation of cellular proteins is inhibited by ALN and LOV (Fig. 1B and 1C, lanes 2 and 7) and that this inhibition is restored by geranylgeraniol (GGOH), an intermediate of the mevalonate pathway, in a concentration-dependent manner (lanes 3-6 and 8-11). Here, recombinant SV40 and adenovirus each carrying the luciferase gene were used to measure their infectivity. As shown in Fig, 1B, SV40 infection was inhibited by both ALN and LOV (lanes 2 and 7). We were puzzled, however, by the finding that GGOH had only a small effect on SV40 infection of ALN-treated cells, whereas it completely rescued SV40 infection of LOV-treated cells (lanes 3-6 and 8-11). Even more puzzling is the observation that adenovirus infection was inhibited by ALN, but not by LOV appreciably (Fig. 1C, lanes 2 and 7), and that GGOH had little effect on adenovirus infection of ALN-treated cells (lanes 3-6). These results suggest that although inhibition of the mevalonate pathway is partly responsible for the suppression of SV40 infection by ALN and LOV, there is a different pathway that is important to infection by these viruses and is targeted by ALN. From the data shown in Fig. 1D, IC50 for the antiviral effect of ALN was calculated to be 8.3 μM.

To gain more insight into the additional pathway, we tested another N-BP, ZOL (Fig. 1A), and an NN-BP, ETI (Fig. 1A), for their effects on adenovirus infection by determining the expression level of the adenovirus E1A protein (Fig. 2A). Consistent with the knowledge that NN-BPs exert their pharmacological effects without inhibiting the mevalonate pathway (Coxon et al., 2000), prenylation of Rap1A was inhibited by ALN and ZOL, but not by ETI appreciably (lanes 3-5). Nonetheless, these drugs were equally effective in inhibiting adenovirus infection (lanes 3-5), and GGOH did not rescue the inhibition by ALN (lane 7). These results were further validated by immunofluorescence staining using anti-E1A antibody,

Molecular Pharmacology Fast Forward. Published on November 10, 2009 as DOI: 10.1124/mol.109.059006
This article has not been copyedited and formatted. The final version may differ from this version.

which showed negligible fluorescence signal from ALN and ETI-treated cells exposed to adenovirus (Fig. 2B). It is therefore likely that adenovirus infection is suppressed through a prenylation-independent pathway not only by N-BPs but also by NN-BPs, which are considered to be structurally similar to, but functionally distinct from, N-NPs.

Identification of DYN2 and SNX9 as ALN-binding proteins. The above finding suggests that these drugs have common cellular targets other than FPPS. To identify such targets, we carried out an affinity purification of ALN-binding proteins from extracts of rat macrophage cells RAW264.7 using high performance latex beads (Shimizu et al., 2000) conjugated with ALN. Consequently, two proteins, one of 100 kD and the other 70 kD, were found to bind specifically to ALN-conjugated beads (Fig. 3A). Sequence analysis by Q-TOF MS revealed that the 100 kD and 70 kD proteins are DYN2, a factor important in various types of endocytic pathways (Takei et al., 1995; Mayor and Pagano, 2007), and SNX9, a factor that interacts with dynamin and regulates its assembly during endocytosis (Lundmark and Carlsson, 2003; Soulet et al., 2005), respectively. The identities of these proteins were confirmed by immunoblotting using their respective antibodies (Fig. 3B). Next, recombinant DYN2 (rDYN2) and SNX9 (rSNX9) proteins were overexpressed in insect cells and *E. coli*, respectively, and the binding of these proteins to ALN-conjugated beads was examined. As shown in Fig. 3C, rDYN2 bound to the beads independently of rSNX9, whereas rSNX9 only bound in the presence of rDYN2, indicating that ALN bound to DYN2 directly and that SNX9 was co-purified by associating with DYN2.

Next, binding specificity was examined by adding free ALN, ZOL, or ETI (Fig. 3D). All three drugs led to the release of both rDYN2 and rSNX9 from the beads in a concentration-dependent manner, suggesting that both N-BPs and NN-BPs can target DYN2. These data are consistent with DYN2 being a molecular target of BPs in adenovirus infection.

ALN reverses lipid-mediated enhancement of DYN2 GTPase activity through competitive binding to DYN2. Dynamins are large GTPases that mediate many forms of endocytosis (Mayor and Pagano, 2007), and their GTPase activity is stimulated upon binding

Molecular Pharmacology Fast Forward. Published on November 10, 2009 as DOI: 10.1124/mol.109.059006
This article has not been copyedited and formatted. The final version may differ from this version.

to lipid membranes (Praefcke et al., 2004). Thus we examined whether ALN has any effect on DYN2 GTPase, using recombinant (r) DYN2 and lipid prepared from bovine brain. In the absence of lipid, ALN had negligible effect on GTP hydrolysis to GDP by rDYN2 at the concentrations examined (Fig. 4A). Lipid stimulated rDYN2 GTPase activity three-fold, and ALN reversed lipid-mediated enhancement of the GTPase activity. Since ALN binds to magnesium ions very well, its inhibitory effect could be due to chelation of magnesium ions in the reactions. To exclude the possibility, we increased the magnesium concentration from 1 mM to 2 mM. As a result, there was no appreciable change in the inhibitory effect of 500 μM ALN.

Given the finding that ALN inhibited the GTPase activity only partially even at the highest concentration examined, we speculated that ALN inhibits only the lipid-activated fraction of DYN2, possibly through competitive binding of ALN and lipid to DYN2. As shown in Fig. 4B, rDYN2 binding to ALN-fixed beads were indeed inhibited by increasing concentrations of lipid. Collectively, these results suggest that ALN reverses lipid-mediated enhancement of DYN2 GTPase activity through competitive binding to DYN2.

ALN binds to DYN2 through its phosphoinositide lipid-binding PH domain. DYN2 is composed of the GTPase domain, the middle domain, the lipid-binding PH domain, the GTPase effector domain (GED), and the proline-arginine-rich domain (PRD) (Schmid et al., 1998; Artalejo et al., 1997). We carried out ALN binding assays using a series of DYN2 mutants and found that its GST-tagged PH domain (GST-PH) binds to ALN, although somewhat weakly (Fig. 5A). As the DYN2 PH domain is known to bind preferentially to acidic phospholipid (Catimel et al., 2009), synthetic lipid composed of phosphatidylcholine (PC) or PC and phosphatidylinositol (3,4,5)-triphosphate (PIP_3) (9:1) was used instead of native lipid as competitors of ALN binding assays. Consequently, PIP_3-containing lipid was found to inhibit rDYN2 or GST-PH binding to ALN efficiently (Fig. 5B). These results led us to conclude that ALN binds to DYN2 through its phosphoinositide lipid-binding PH domain.

ALN, ZOL, and ETI inhibit endocytosis. As DYN2 and its GTPase activity play

Molecular Pharmacology Fast Forward. Published on November 10, 2009 as DOI: 10.1124/mol.109.059006
This article has not been copyedited and formatted. The final version may differ from this version.

important roles in endocytosis, our findings raise the possibility that inhibition of viral infection is due to defective endocytosis. This hypothesis was first tested using a model system. Following incubation of HeLa cells with BPs at 37°C for 4 h, uptake of fluorescently labeled transferrin, which is a marker of the clathrin-mediated pathway, was measured by flow cytometry and fluorescence confocal microscopy. Our results show that, in the presence of ALN, ZOL or ETI, transferrin uptake was significantly decreased and that the suppression level was similar to that in the presence of chlorpromazine (CPZ), a clathrin-dependent endocytosis inhibitor (Fig. 6).

ALN inhibits liposome vesiculation in vitro and scission of endocytic vesicles in adenovirus-infected cells. Dynamins self-assemble into ring-like complexes to carry out vesicle scission by tubulation and severance of lipid membranes using GTP hydrolysis as source of energy (Mayor and Pagano, 2007). This activity can be reconstituted in vitro using purified rDYN2, which also self-associates and binds to lipid bilayers to form tubular structures (Fig. 7A, +rDYN2, -GTP) that can be constricted to form small lipid vesicles upon GTP addition (+rDYN2, +GTP) (Sweitzer and Hinshaw, 1998). However, this vesiculation activity was inhibited in the presence of ALN (+rDYN2+ALN, +GTP). As this observation is similar to that of a GTPase-deficient mutant rDYN2 (K44A) (Damke et al., 1994), which forms tubular lipid structures but is incapable of vesiculation due to a point mutation in the GTP binding site (+rDYN2 (K44A)), our results strongly suggest that ALN targets the GTPase activity of DYN2 to suppress endocytosis.

HeLa cells infected with adenovirus in the absence or presence of ALN were analyzed by electron microscopy. As shown in Fig. 7B, normal endocytic vesicles containing virus particles are round and found detached from the plasma membrane, whereas in the presence of ALN, these vesicles appear to be trapped near the cytoplasmic membrane. Thus, these observations suggest that the cause of ALN-mediated inhibition of adenovirus infection may be defective scission due to DYN2 GTPase activity inhibition at the neck of the invaginated pit (arrow).

Molecular Pharmacology Fast Forward. Published on November 10, 2009 as DOI: 10.1124/mol.109.059006
This article has not been copyedited and formatted. The final version may differ from this version.

DISCUSSION

In this study, we investigated the effects of BPs on SV40 and adenovirus infections and found that these viruses show different sensitivity toward the various drugs examined. The results obtained using the HMG-CoA reductase inhibitor LOV indicate that prenylation of a certain cellular or viral protein is important to SV40 infection, although the existence of such a protein is not known. On the other hand, the results obtained using ALN and GGOH indicate that ALN exerts its inhibitory effects on viral infection partly or entirely through a mevalonate-independent pathway, most likely through inhibition of DYN2-mediated endocytosis, as our biochemical data suggest here. ALN was found to target DYN2 GTPase activity, leading to its inability to pinch off endocytic vesicles. Moreover, DYN2 was found to be targeted by ETI, an NN-BP that is not known to target FPPS, which further supports our discovery of an additional non-mevalonate-related inhibitory mechanism for BPs. Adenovirus infection requires DYN2 in clathrin-dependent endocytosis, and expression of the GTPase-deficient mutant DYN2 (K44A) significantly reduces infectivity (Wang et al., 1998). SV40 enters cells via caveolar endocytosis (Anderson et al., 1996), a clathrin-independent but DYN2-dependent pathway. Thus, our identification of DYN2 as a target for antiviral activity of BPs is consistent with its key role in multiple endocytic pathways.

It may be surprising that using ALN as ligand, a highly charged molecule, DYN2 was purified almost exclusively. We have carried out a number of affinity purifications using various low molecular-weight compounds as ligands. In some cases, numerous proteins were obtained in initial experiments, and subsequent optimization of various parameters, such as the amount of ligand immobilized, composition of binding and washing buffers, and elution conditions (e.g., competitive elution using free ligand), was necessary. But in the other cases, only one or a few proteins were isolated without the need for extensive optimization, leading to rapid identification of relevant molecular targets (reviewed in Sakamoto et al., 2009). In principle, relative abundance of affinity-purified proteins are determined by the concentration of each protein in input material and its equilibrium dissociation constant for the ligand. Hence, a simple interpretation of our data is that there was sufficient difference in Kd

Molecular Pharmacology Fast Forward. Published on November 10, 2009 as DOI: 10.1124/mol.109.059006
This article has not been copyedited and formatted. The final version may differ from this version.

between DYN2 binding and other “nonspecific” binding that might have occurred through ionic interactions. Besides, while it is not central to the discussion here, we believe that a key to success is the use of affinity beads called SG beads and FG beads, which we have developed over decades (Sakamoto et al., 2009). They are spherical organic-polymer particles of approximately 200 nm in diameter, which is two-to-three orders of magnitude smaller than the diameter of typical agarose beads. Their nonporous structure, large surface area per weight, and moderately hydrophilic surface appear to contribute to a high signal-to-background ratio in purification.

Below we discuss the possibility that clinically relevant doses of BPs contribute to treatments of diseases other than blocking bone loss. On the one hand, we determined IC50 for the antiviral effect of ALN to be 8.3 μM (Fig. 1D). On the other hand, it is generally accepted that following bisphosphonate administration, a fraction of the drug becomes incorporated into the skeleton whereas the remainder is cleared rapidly from the blood to the urine (Russell et al., 2007). Following single oral administration of 70 mg of ALN to humans, its elimination half-life is 1.67 h and the maximum plasma concentration is 41 ng/ml or 0.16 μM, (Yum & Kwon, 2006). It is therefore unlikely that by the regimen used in the study, plasma concentrations of ALN come close to the level that affects DYN2-mediated endocytosis. However, a few studies have shown that some of the drug also accumulates temporarily in soft tissues, such as liver and spleen, and is subsequently released over a period of days (Stepensky et al., 2003), although its precise pharmacokinetics remains to be determined. In another study, it is suggested that bisphosphonate concentrations at the aorta are much higher (up to 24 fold) than plasma levels (Ylitalo et al., 1996). In addition, the deposition in soft tissues may vary by the mode of drug administration (Stepensky et al., 2003). Furthermore, bisphosphonates are generally safe and well tolerated even at higher doses; for example, Paget's disease patients receive up to 400 mg of bisphosphonates per day. In summary, local tissue concentrations of bisphosphonates may be higher than their plasma concentrations, and even higher local concentrations may be achieved by considering pharmaceutical formulations and mode of administration. For these reasons, we consider that our present findings may have potential clinical implications.

BPs have been prescribed for over three decades in the treatment of bone diseases and are currently the most widely employed bone resorption drugs. BPs mainly target osteoclasts, but can also affect other cell types in various ways, including the suppression of proliferation, adhesion, migration, and invasion of tumor cells (Roelofs et al., 2006). Interestingly, the new BP target found here, DYN2, also plays diverse cellular roles. DYN2 is most famous for its role in membrane scission, the last step required to release invaginated endocytic vesicles into the cytoplasm (Mayor and Pagano, 2007; Marks et al., 2001). Hence, in addition to reducing osteoclast bone uptake indirectly through the inhibition of prenylation, N-BPs may also directly stop resorption in vivo by mechanically blocking the severance and release of loaded vesicles into the cytoplasm of osteoclasts, as our data suggest here. Furthermore, reports by others have shown that DYN2 also plays important roles in actin remodeling and the formation of podosomes, thus suggesting that BPs may also affect the motility of osteoclasts and how these cells secure contact between the membrane and the extracellular matrix (Bruzzaniti et al., 2005), which may also explain their effects on tumor cells.

Through the discovery of DYN2 as a target of BPs, this study has uncovered a previously unknown mechanism of action of BPs and offers potential novel use for these drugs. Our findings will likely be extendable to research on other viruses. One example is HIV-1, the infectivity of which is known to be enhanced by DYN2 (Pizzato et al., 2004). However, due to the complexity of the various pathways employed by viruses to enter cells and the various cellular roles played by DYN2, much work is still needed to clarify how different viruses respond to BP treatments. Incidentally, investigations or trials of alternative uses of BPs, such as studies on the inhibition of growth of human T-cell leukemia virus type I-infected T-cell lines (Ishikawa et al., 2007) or the treatment of HIV-associated osteoporosis (Negredo et al., 2005; Qaqish and Sims, 2004), are emerging. The knowledge gained through these efforts may lead to better antiviral therapies through effective combinatorial treatments using new and old strategies.

Molecular Pharmacology Fast Forward. Published on November 10, 2009 as DOI: 10.1124/mol.109.059006
This article has not been copyedited and formatted. The final version may differ from this version.

ACKNOWLEDGMENTS

We are grateful to Dr. Kazuhisa Nakayama (Kyoto University) for providing the DYN2 cDNA and to Dr. Hiroyuki Kouji (Institute for Life Science Research, Asahi Chemical Industry Co. Ltd.) for providing biosphosphonates.

Molecular Pharmacology Fast Forward. Published on November 10, 2009 as DOI: 10.1124/mol.109.059006
This article has not been copyedited and formatted. The final version may differ from this version.

REFERENCES

Anderson HA, Chen Y, and Norkin LC (1996) Bound simian virus 40 translocates to caveolin-enriched membrane domains, and its entry is inhibited by drugs that selectively disrupt caveolae. *Mol Biol Cell* **7:**1825-1834.

Artalejo CR, Lemmon MA, Schlessinger J, and Palfrey HC (1997) Specific role for the PH domain of dynamin-1 in the regulation of rapid endocytosis in adrenal chromaffin cells. *EMBO J* **16:**1565-1574.

Bordier BB, Marion PL, Ohashi K, Kay MA, Greenberg HB, Casey JL, and Glenn JS (2002) A prenylation inhibitor prevents production of infectious hepatitis delta virus particles. *J Virol* **76:**10465-10472.

Bruzzaniti A, Neff L, Sanjay A, Horne WC, De Camilli P, and Baron R (2005) Dynamin forms a Src kinase-sensitive complex with Cbl and regulates podosomes and osteoclast activity. *Mol Biol Cell* **16:**3301-3313.

Catimel B, Yin MX, Schieber C, Condron M, Patsiouras H, Catimel J, Robinson DE, Wong LS, Nice EC, Holmes AB, and Burgess AW (2009) PI(3,4,5)P3 Interactome. *J Proteome Res.* **8:**3712-3726.

Coxon FP, Helfrich MH, van 't Hof RJ, Sebti SM, Ralston SH, Hamilton AD, and Rogers MJ (2000) Protein geranylgeranylation is required for osteoclast formation, function, and survival: Inhibition by bisphosphonates and GGTI-298. *J Bone Miner Res* **15:**1467-1476.

Damke H, Baba T, Warnock DE, and Schmid SL (1994) Induction of mutant dynamin specifically blocks endocytic coated vesicle formation. *J Cell Biol* **127:**915-934.

Damke H, Muhlberg AB, Sever S, Sholly S, Warnock DE, and Schmid SL (2001) Expression, purification, and functional assays for self-association of dynamin-1. *Methods Enzymol* **329:**447-457.

del Real G, Jiménez-Baranda S, Mira E, Lacalle RA, Lucas P, Gómez-Moutón C, Alegret M, Peña JM, Rodríguez-Zapata M, Alvarez-Mon M, Martínez-A C, and Mañes S (2004) Statins inhibit HIV-1 infection by down-regulating Rho activity. *J Exp Med* **200:**541-547.

Dignam JD, Lebovitz RM, and Roeder RG (1983) Accurate transcription initiation by RNA polymerase II in a soluble extract from isolated mammalian nuclei. *Nucleic Acids Res*

11:1475-1489.

Dunford JE, Rogers MJ, Ebetino FH, Phipps RJ, and Coxon FP (2006) Inhibition of protein prenylation by bisphosphonates causes sustained activation of Rac, Cdc42, and Rho GTPases. *J Bone Miner Res* **21:**684-694.

Einav S and Glenn JS (2003) Prenylation inhibitors: a novel class of antiviral agents. *J Antimicrob Chemother* **52:**883-886.

Farassati F, Yang AD, and Lee PW (2001) Oncogenes in Ras signalling pathway dictate host-cell permissiveness to herpes simplex virus 1. *Nat Cell Biol* **3:**745-750.

Frith JC and Rogers MJ (2003) Antagonistic effects of different classes of bisphosphonates in osteoclasts and macrophages in vitro. *J Bone Miner Res* **18:**204-212.

Glenn JS, Marsters JC, and Greenberg HB (1998) Use of a prenylation inhibitor as a novel antiviral agent. *J Virol* **72:**9303-9306.

Gower TL and Graham BS (2001) Antiviral activity of lovastatin against respiratory syncytial virus in vivo and in vitro. *Antimicrob Agents Chemother* **45:**1231-1237.

Heymann D, Ory B, Gouin F, Green JR, and Rédini F (2004) Bisphosphonates: new therapeutic agents for the treatment of bone tumors. *Trends Mol Med* **10:**337-343.

Ishikawa C, Matsuda T, Okudaira T, Tomita M, Kawakami H, Tanaka Y, Masuda M, Ohshiro K, Ohta T, and Mori N (2007) Bisphosphonate incadronate inhibits growth of human T-cell leukaemia virus type I-infected T-cell lines and primary adult T-cell leukaemia cells by interfering with the mevalonate pathway. *Br J Haematol* **136:**424-432.

Lundmark R and Carlsson SR (2003) Sorting nexin 9 participates in clathrin-mediated endocytosis through interactions with the core components. *J Biol Chem* **278:**46772-46781.

Marks B, Stowell MH, Vallis Y, Mills IG, Gibson A, Hopkins CR, and McMahon HT (2001) GTPase activity of dynamin and resulting conformation change are essential for endocytosis. *Nature* **410:**231-235.

Mayor S and Pagano RE (2007) Pathways of clathrin-independent endocytosis. *Nat Rev Mol Cell Biol* **8:**603-612.

Nakanishi A, Chapellier B, Maekawa N, Hiramoto M, Kuge T, Takahashi RU, Handa H, and

Imai T (2008) SV40 vectors carrying minimal sequence of viral origin with exchangeable capsids. *Virology* **379:**110-117.

Negredo E, Martínez-López E, Paredes R, Rosales J, Pérez-Alvarez N, Holgado S, Gel S, del Rio L, Tena X, Rey-Joly C, and Clotet B (2005) Reversal of HIV-1-associated osteoporosis with once-weekly alendronate. *AIDS* **19:**343-345.

Pizzato M, Helander A, Popova E, Calistri A, Zamborlini A, Palù G, and Göttlinger HG (2004) Dynamin 2 is required for the enhancement of HIV-1 infectivity by Nef. *Proc Natl Acad Sci U S A* **104:**6812-6817.

Praefcke GKJ and McMahon HT (2004) The dynamin superfamily: universal membrane tubulation and fission molecules? *Nat Rev Mol Cell Biol* **5:**133-146.

Qaqish RB and Sims KA (2004) Bone disorders associated with the human immunodeficiency virus: pathogenesis and management. *Pharmacotherapy* **24:**1331-1346.

Reszka AA, Halasy-Nagy JM, Masarachia PJ, amd Rodan GA (1999) Bisphosphonates act directly on the osteoclast to induce caspase cleavage of mst1 kinase during apoptosis. A link between inhibition of the mevalonate pathway and regulation of an apoptosis-promoting kinase. *J Biol Chem* **274:**34967-34973.

Roelofs AJ, Thompson K, Gordon S, and Rogers MJ (2006) Molecular mechanisms of action of bisphosphonates: current status. *Clin Cancer Res* **12:**6222-6230.

Russell RG, Xia Z, Dunford JE, Oppermann U, Kwaasi A, Hulley PA, Kavanagh KL, Triffitt JT, Lundy MW, Phipps RJ, Barnett BL, Coxon FP, Rogers MJ, Watts NB, and Ebetino FH (2007) Bisphosphonates: an update on mechanisms of action and how these relate to clinical efficacy. *Ann N Y Acad Sci* **1117:**209-257.

Sakamoto S, Kabe Y, Hatakeyama M, Yamaguchi Y, and Handa H. (2009) Development and application of high-performance affinity beads: toward chemical biology and drug discovery. *Chem Rec* **9:**66-85.

Schmid SL, McNiven MA, and De Camilli P (1998) Dynamin and its partners: a progress report. *Curr Opin Cell Biol* **10:**504-512.

Shimizu N, Sugimoto K, Tang J, Nishi T, Sato I, Hiramoto M, Aizawa S, Hatakeyama M, Ohba R, Hatori H, Yoshikawa T, Suzuki F, Oomori A, Tanaka H, Kawaguchi H, Watanabe

H, and Handa H (2000) High-performance affinity beads for identifying drug receptors. *Nat Biotechnol* **18:**877-881.

Soulet F, Yarar D, Leonard M, and Schmid SL (2005) SNX9 regulates dynamin assembly and is required for efficient clathrin-mediated endocytosis. *Mol Biol Cell* **16:**2058-2067.

Stepensky D, Kleinberg L, and Hoffman A. (2003) Bone as an effect compartment : models for uptake and release of drugs. *Clin Pharmacokinet* **42:**863-881.

Sweitzer SM and Hinshaw JE (1998) Dynamin undergoes a GTP-dependent conformational change causing vesiculation. *Cell* **93:**1021-1029.

Takei K, McPherson PS, Schmid SL, and De Camilli P (1995) Tubular membrane invaginations coated by dynamin rings are induced by GTP-gamma S in nerve terminals. *Nature* **374:**186-190.

van Beek ER, Cohen LH, Leroy IM, Ebetino FH, Löwik CW, and Papapoulos SE (2003) Differentiating the mechanisms of antiresorptive action of nitrogen containing bisphosphonates. *Bone* **33:**805-811.

Wang K, Huang S, Kapoor-Munshi A, and Nemerow G (1998) Adenovirus internalization and infection require dynamin. *J Virol* **72:**3455-3458.

Ylitalo R, Monkkonen J, Urtti A, and Ylitalo P (1996) Accumulation of bisphosphonates in the aorta and some other tissues of healthy and atherosclerotic rabbits. *J Lab Clin Med* **127:**200-206.

Yun MH and Kwon KI (2006) High-performance liquid chromatography method for determining alendronate sodium in human plasma by detecting fluorescence: application to a pharmacokinetic study in humans. *J Pharm Biomed Anal* **40:**168-172.

FOOTNOTES

This study was supported in part by Special Coordination Funds for Promoting Science and Technology from the Japan Science and Technology Agency (KH217001) and by a Grant from the Global COE Program from the Ministry of Education, Culture, Sports, Science and Technology of Japan (A-04).

Molecular Pharmacology Fast Forward. Published on November 10, 2009 as DOI: 10.1124/mol.109.059006
This article has not been copyedited and formatted. The final version may differ from this version.

FIGURE LEGENDS

Fig. 1. Inhibition of viral infections by ALN through a prenylation-independent pathway. A, Molecular structures of ALN, ZOL, and ETI. B and C, 293FT cells were treated with various compounds (100 μM ALN, 10 μM LOV, or the indicated concentrations of GGOH) and then infected with recombinant SV40 or adenovirus each carrying the luciferase gene. Cell lysates were subjected to luciferase assays and immunoblotting. Luciferase activity was normalized to the activity of lane 1. Data represent the means ± standard deviations of nine (lanes 1 to 6) or six (lanes 7 to 11) independent experiments. *, $p < 0.01$ (Mann-Whitney *U* test). D, 293FT cells were treated with various concentrations of ALN (0.4 to 300 μM) and then infected with recombinant adenovirus carrying the luciferase gene. Luciferase activity was measured, normalized to the activity obtained in the absence of ALN, and plotted against logarithmic concentrations of ALN. Data represent the means ± standard deviations of three independent experiments. The correlation coefficient is shown in the inset.

Fig. 2. Inhibition of adenoviral infection by ALN, ZOL, and ETI. A, HeLa cells were treated with the indicated compounds and then infected with adenovirus. Cell lysates were immunoblotted with the indicated antibodies. B, Fluorescence microscopy of adenovirus-infected cells. E1A and DNA were visualized with anti-E1A antibody and 4',6-diamidino-2-phenylindole (DAPI), respectively.

Fig. 3. Identification of DYN2 and SNX9 as ALN-binding proteins. A and B, ALN-conjugated beads (+) or control beads (-) were incubated with RAW264.7 cell extract. Bound proteins were subjected to SDS-PAGE followed by silver staining (A) or immunoblotting using anti-DYN2 or anti-SNX9 antibodies (B). C and D, Interactions of ALN with recombinant proteins. rDYN2 and/or rSNX-9 (1.2 μM each) were incubated with ALN-conjugated (+) or control (-) beads. Input and eluate materials were analyzed by SDS-PAGE and silver staining. In D, cell extract was incubated with free ALN, ZOL, or ETI as indicated, prior to binding to ALN-conjugated beads.

Molecular Pharmacology Fast Forward. Published on November 10, 2009 as DOI: 10.1124/mol.109.059006
This article has not been copyedited and formatted. The final version may differ from this version.

Fig. 4. ALN reverses lipid-mediated enhancement of DYN2 GTPase activity through competitive binding to DYN2. A, GTPase activity of rDYN2 was assayed in the absence or presence of ALN and SUVs prepared from bovine brain. Data represent the means ± standard deviations of six independent experiments. *, $p < 0.01$ (Mann-Whitney *U* test). B, DYN2-ALN interactions were examined using ALN-conjugated beads and rDYN2 as in Fig. 3C, except that the beads were preincubated with various amounts of SUVs prepared from bovine brain.

Fig. 5. ALN binds to DYN2 through its phosphoinositide lipid-binding PH domain. Recombinant DYN2 or its GST-tagged mutants, schematically shown at the top, were subjected to ALN-binding assays. In B, SUVs composed of PC or PC/PIP_3 (9:1) were added to binding reactions as competitors. Aliquots of input (A) and eluate (A, B) materials were analyzed by SDS-PAGE and silver staining.

Fig. 6. ALN, ZOL, and ETI inhibit endocytosis. HeLa cells were incubated with Alexa-Fluor-546 transferrin or left untreated (unlabeled). Prior to transferrin uptake, cells were treated with CPZ, ALN, ZOL, or ETI, or left untreated (non-treated). Incorporation of the fluorescent dye was examined by FACS (left) and fluorescence confocal microscopy (right). The incorporation level in non-treated cells and in drug-treated cells are indicated by arrows.

Fig. 7. ALN inhibits DYN2-dependent liposome vesiculation. A, SUVs prepared from bovine brain were incubated with wild-type rDYN2 or its GTPase-deficient mutant K44A in the presence or absence of ALN and GTP as indicated. Electron micrographs of negatively stained SUVs were taken. Scale bar, 1 μm. B, Defective scission of endocytic vesicles in adenovirus-infected HeLa cells in the presence of ALN. Electron micrographs of ultrathin sections of adenovirus-infected cells were taken without or with prior ALN treatment. Scale bar, 500 nm. “Ad” indicates adenovirus particles and arrow indicates the neck of the invaginated pit.

Fig. 1

Molecular Pharmacology Fast Forward. Published on November 10, 2009 as DOI: 10.1124/mol.109.059006
This article has not been copyedited and formatted. The final version may differ from this version.

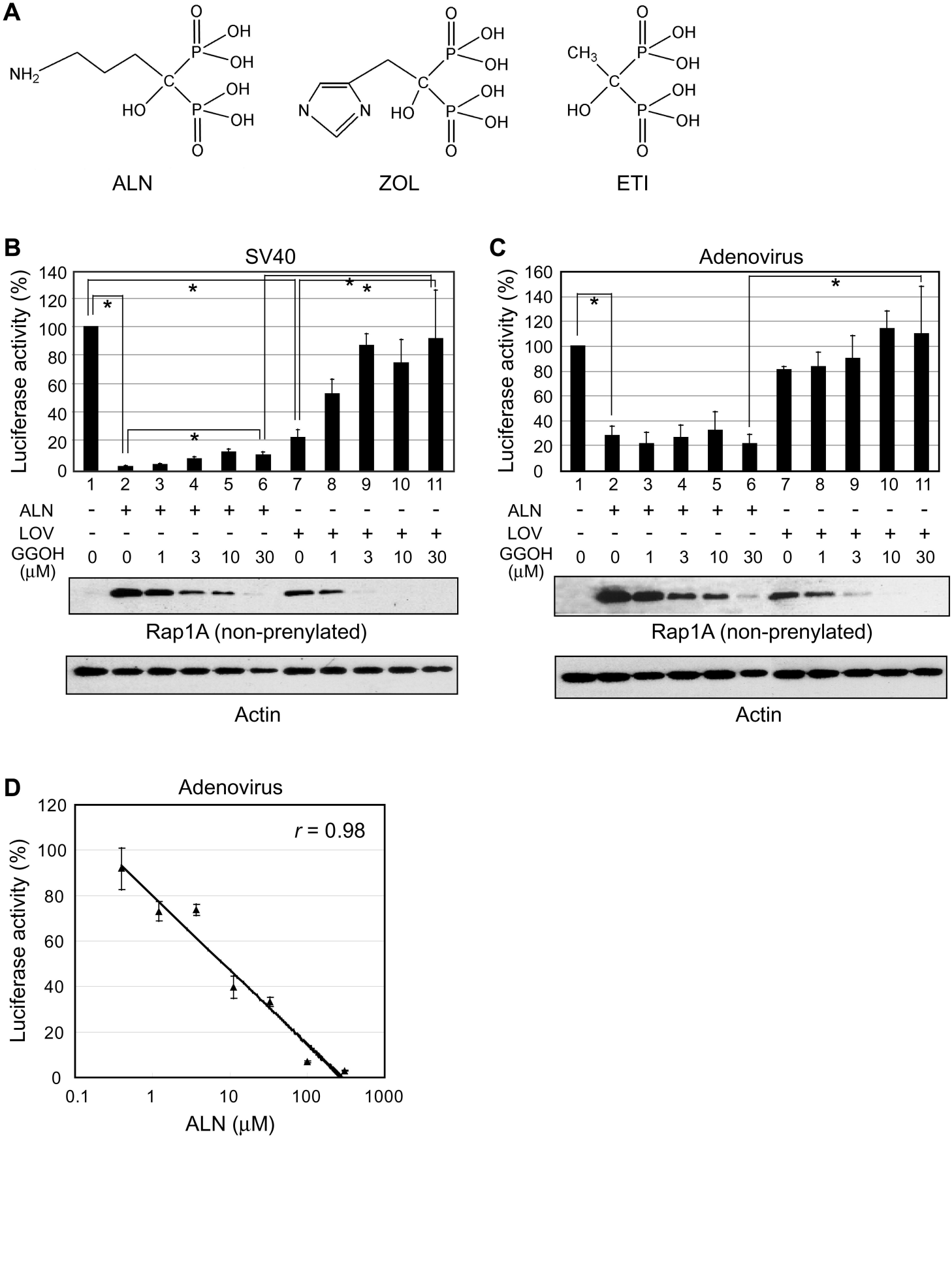

Fig. 2

Molecular Pharmacology Fast Forward. Published on November 10, 2009 as DOI: 10.1124/mol.109.059006
This article has not been copyedited and formatted. The final version may differ from this version.

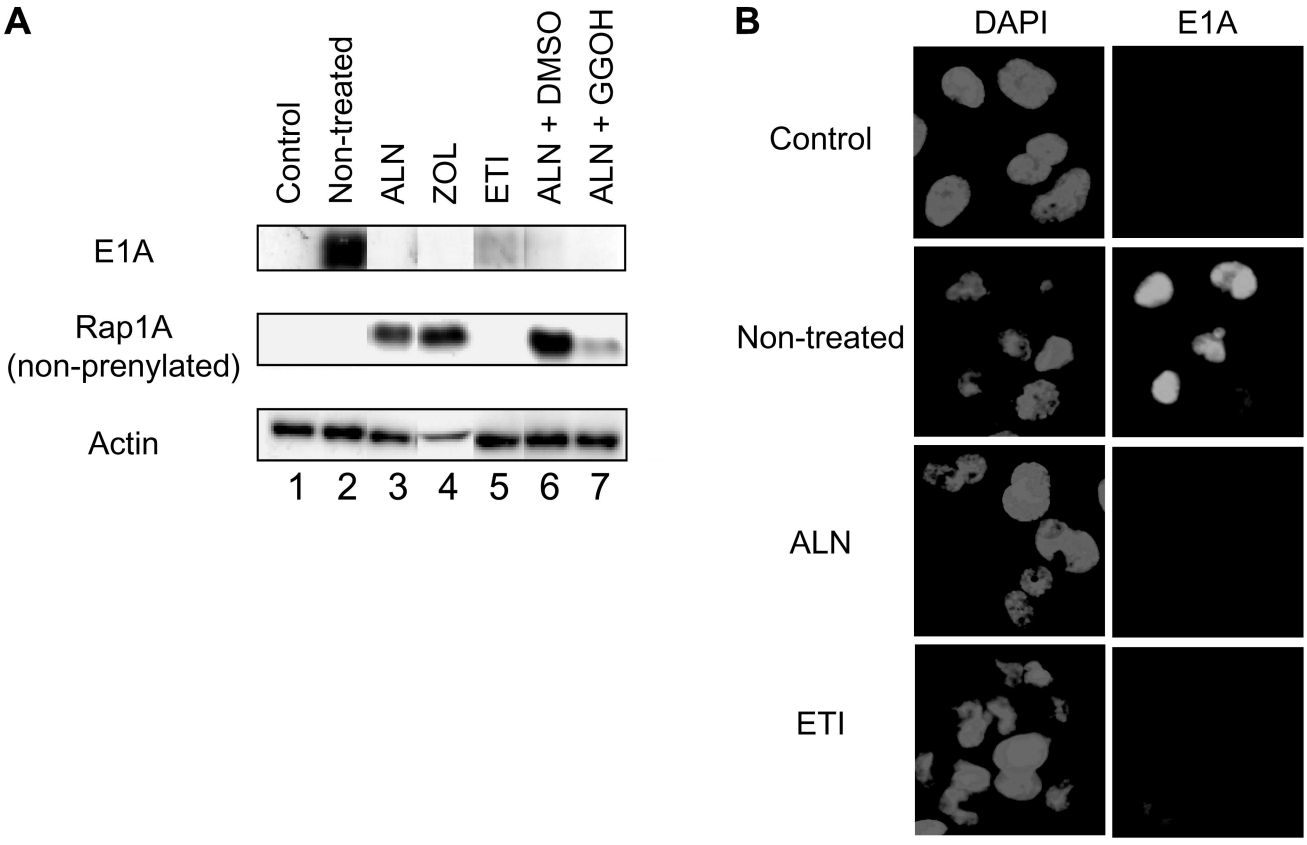

Fig. 3

Molecular Pharmacology Fast Forward. Published on November 10, 2009 as DOI: 10.1124/mol.109.059006
This article has not been copyedited and formatted. The final version may differ from this version.

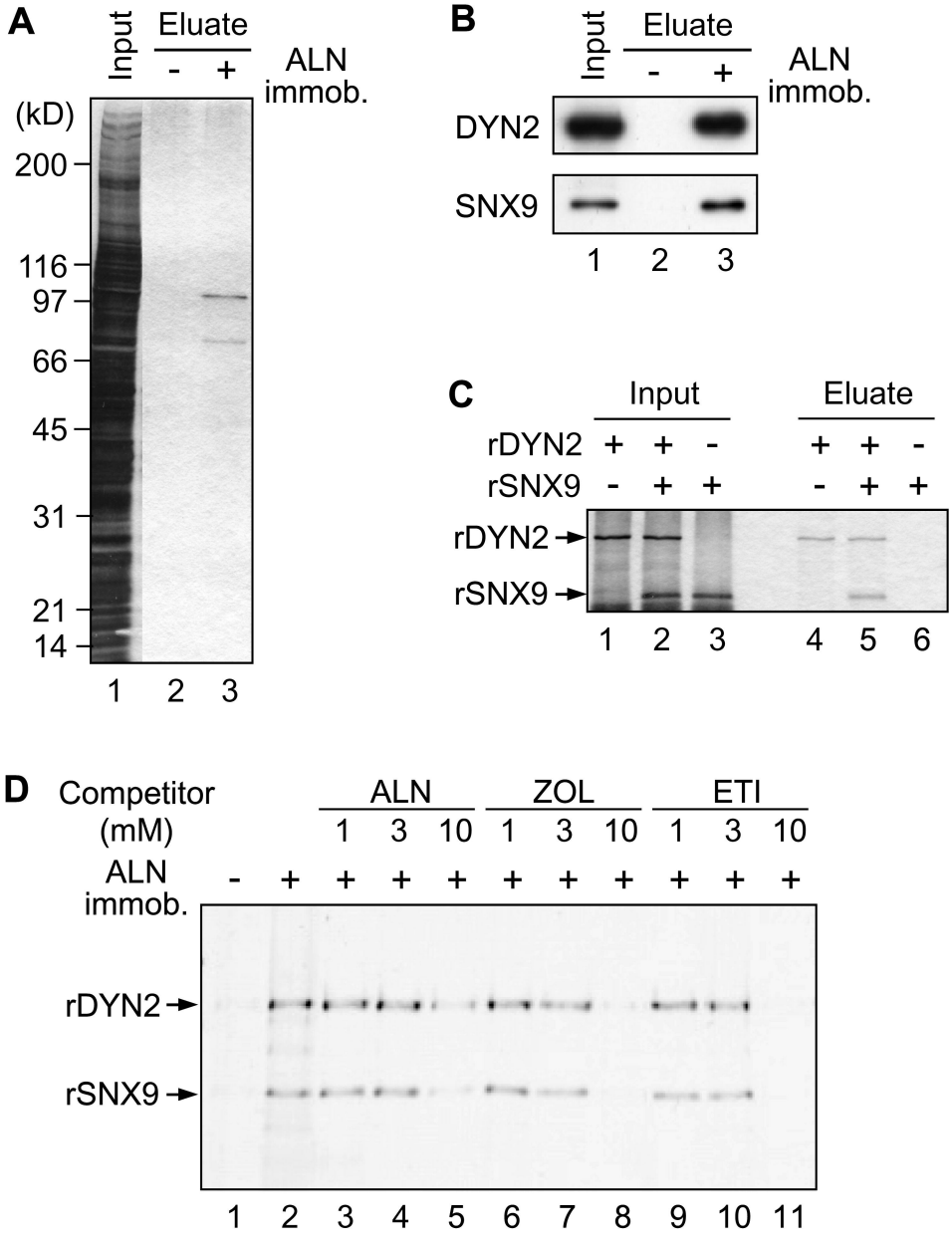

Fig. 4

Molecular Pharmacology Fast Forward. Published on November 10, 2009 as DOI: 10.1124/mol.109.059006
This article has not been copyedited and formatted. The final version may differ from this version.

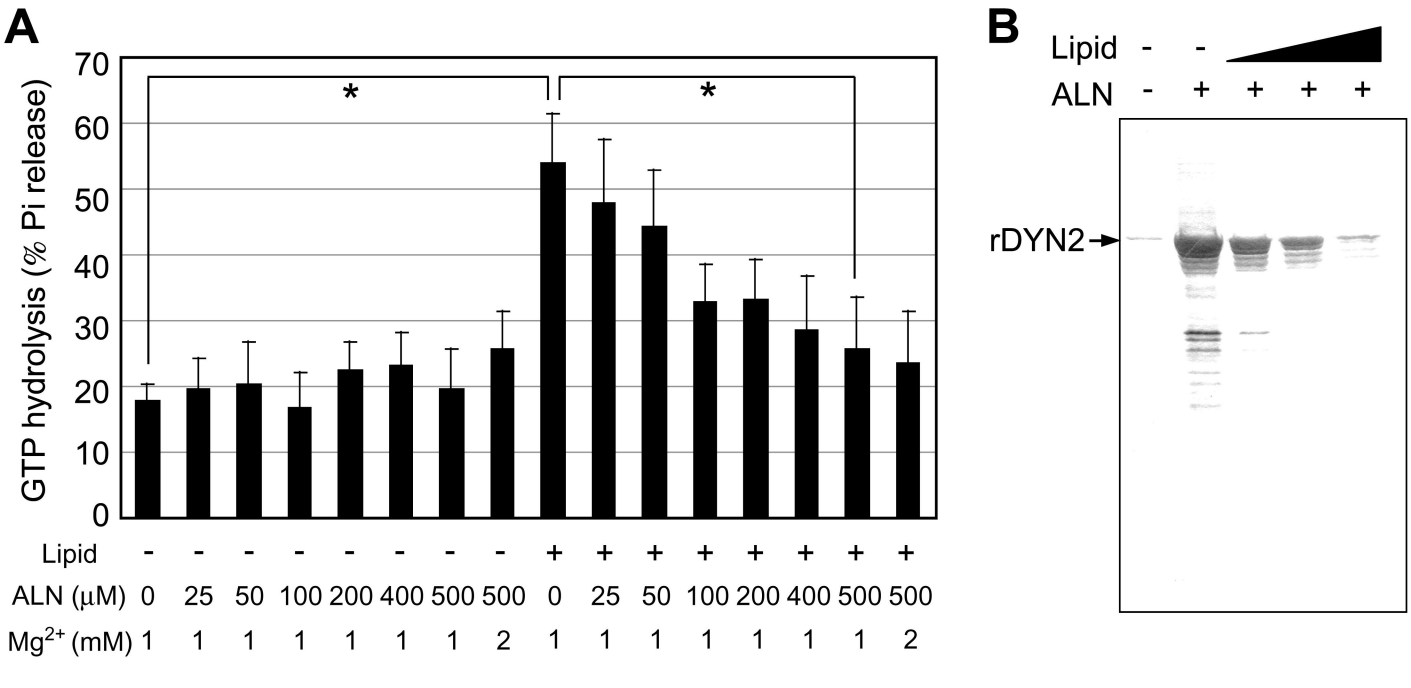

Fig. 5

Molecular Pharmacology Fast Forward. Published on November 10, 2009 as DOI: 10.1124/mol.109.059006
This article has not been copyedited and formatted. The final version may differ from this version.

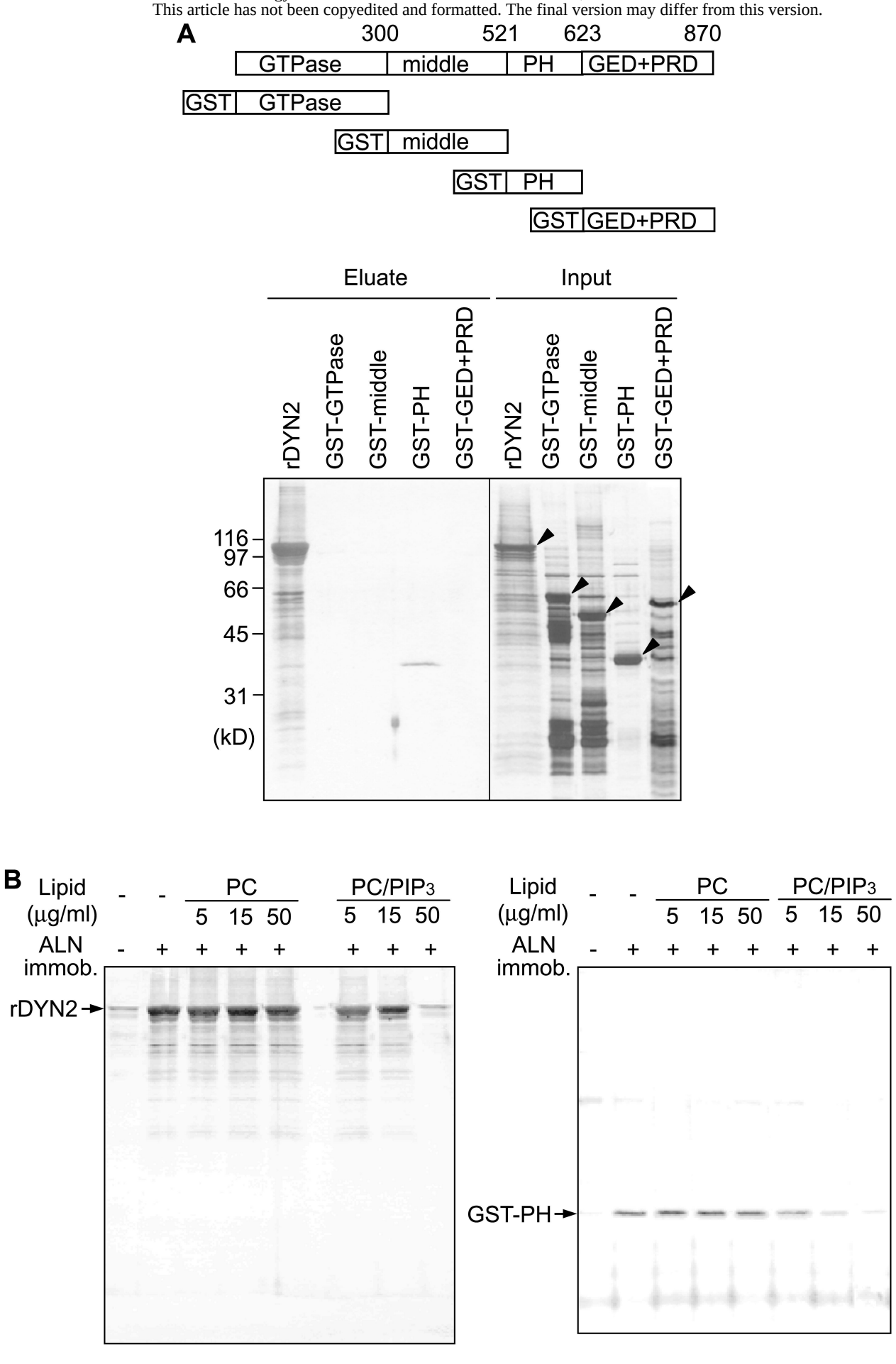

Fig. 6

Molecular Pharmacology Fast Forward. Published on November 10, 2009 as DOI: 10.1124/mol.109.059006
This article has not been copyedited and formatted. The final version may differ from this version.

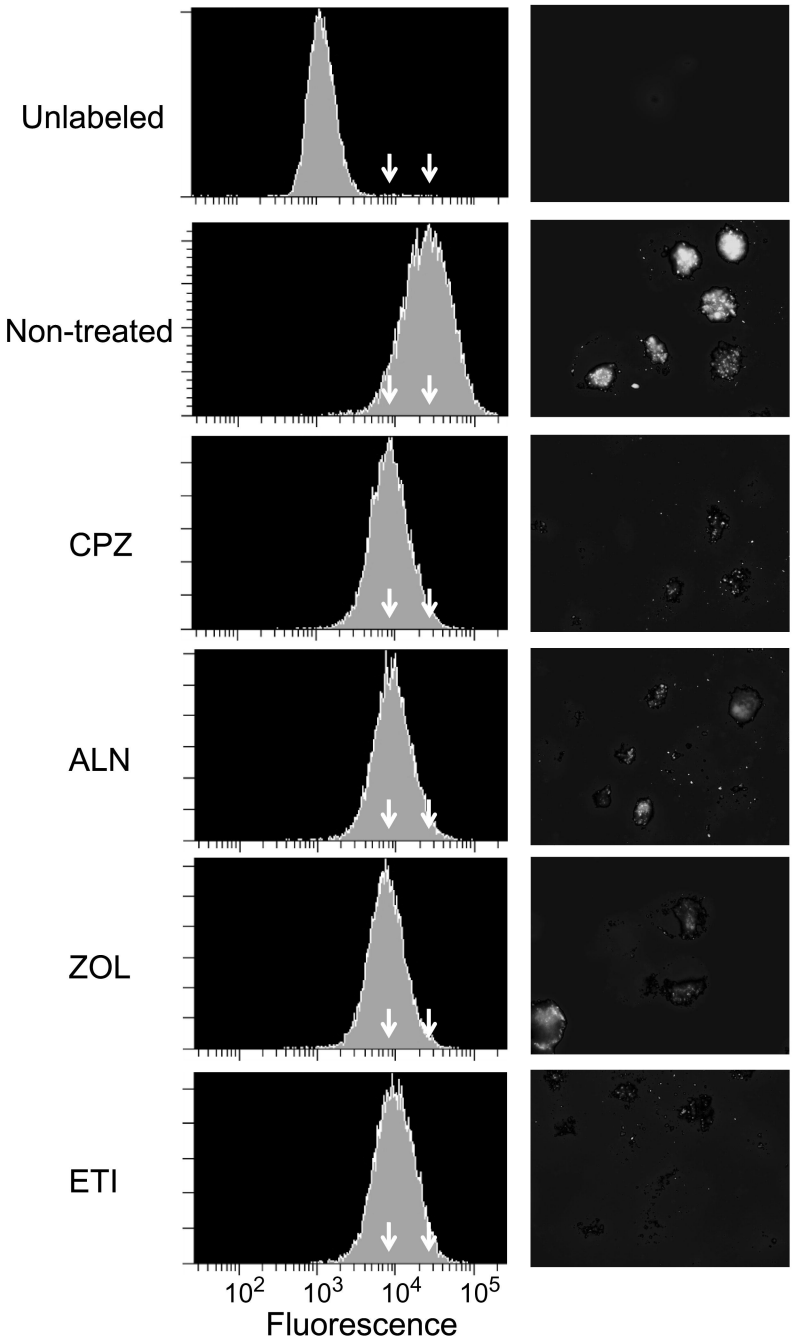

Fig. 7

Molecular Pharmacology Fast Forward. Published on November 10, 2009 as DOI: 10.1124/mol.109.059006
This article has not been copyedited and formatted. The final version may differ from this version.